

Supporting Online Material for

Facile preparation and ultra-microporous structure of melamine-resorcinol-formaldehyde polymeric microspheres

Huanhuan Zhou, Shen Xu, Haiping Su, Mei Wang Wenming Qiao, Licheng Ling and Donghui

Long*

State Key Laboratory of Chemical Engineering, East China University of Science and Technology,
Shanghai 200237

*To whom correspondence should be addressed. E-mail: longdh@ecust.edu.cn

This PDF file includes:

Experimental details

Figs. S1 to S3

Table S1 to S3

References

1. Experimental details

1.1 Materials

All starting materials were purchased from Sinopharm Co. and used without further purification.

1.2 Preparation of the MRF microspheres

The MRF microspheres were synthesized via a hydrothermal method by using melamine, resorcinol and formaldehyde solution as precursors. In a typical synthesis of the MRF-1 microspheres with the total concentration of 15 g/100mL, 3.87 g resorcinol (35 mmol) and 5.70 g formaldehyde (37 wt. %, 70 mmol) were dissolved in 30 ml of distilled water and then stirred at 40 °C for more than 1 h. Subsequently, 4.43 g melamine (35 mmol) and 8.56 g formaldehyde (37 wt. %, 105 mmol) were dissolved in 30 ml of distilled water at 80 °C with consecutive agitation until the solution became clear. The above solution was cooled down to 40 °C and then added into the RF solution with continually stirred for 30 min. The mixed solution was then transferred to a Teflon-lined autoclave and heated at 120 °C for 24 h under a static condition. The solid product was recovered by filtration and air-dried at 100 °C for 24 h. The typical yields of microspheres per synthesis are around 85%.

The polymer microspheres can be obtained at a hydrothermal temperature ranging from 80 to 180 °C and with a wide reactant concentration (2-20 g/100 ml H₂O) and a wide precursor composition (M/R in the range of 0-6).

1.3 Characterization

Elemental analysis was carried out using Elemental Vario EL III. The carbon (C), hydrogen (H), and nitrogen (N) contents of the carbons were determined directly using the thermal conductivity detector.

The surface composition of the NMC was obtained from an Axis Ultra DLD X-ray photoelectron spectroscopy. The X-ray source operated at 15 kV and 10 mA. The working pressure was lower than 2×10^{-8} Torr (1 Torr = 133.3 Pa). The C_{1s}, N_{1s} and O1s XPS spectra were measured at 0.1 eV step size. The N_{1s} XPS signals were fitted with mixed Lorentzian–Gaussian curves, and a Shirley function was used to subtract the background.

Fourier transform infrared (FTIR) spectra of samples were collected by a Nicolet 5S×C FTIR system. Each sample was first finely ground and then diluted with KBr to give a KBr/MRF weight ratio of 200. The FTIR spectra were recorded by accumulating 400 scans at a spectra resolution of 2cm^{-1} .

High-resolution solid-state ^{13}C nuclear magnetic resonance (NMR) experiments were carried out on a JEOL ECA400 spectrometer operated at 100.53 MHz using the single-pulse decoupling method.

The morphologies of samples were observed under scanning electron microscopy (SEM, JEOL 7100F) .

Nitrogen adsorption/desorption isotherms were measured at 77 K with a Quadrasorb SI analyser. Before the measurements, the samples were degassed in vacuum at 473 K for 12 h. The Brunauer-Emmett-Teller (BET) method was utilized to calculate the specific surface area.

CO₂ adsorption isotherms were measured at 273 and 298 K with a Quadrasorb SI analyser. Before the measurements, the samples were degassed in vacuum at 373 K for 12 h. The Brunauer-Emmett-Teller (BET) and DFT methods were utilized to calculate the specific surface area. The pore size distributions were calculated using the non-local DFT model.

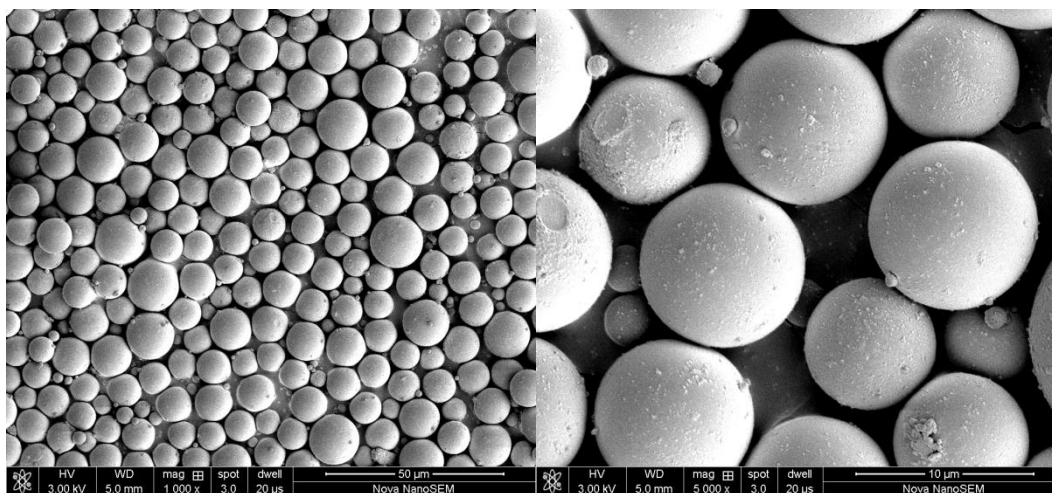


Fig.S1 SEM images of MF microspheres. Compared to the MRF microspheres, the MF microspheres show large particle size. In addition, the RF microspheres are dark red in color and the MF microspheres are pure white, while the color of the MRF microspheres is highly dependent on the M/F ratio and gradually changes from red to pale with the increase of M/F ratio. All the MRF products are uniform in particle size and homogenous in color, basically excluding the possible of forming the mixture of MF and RF.

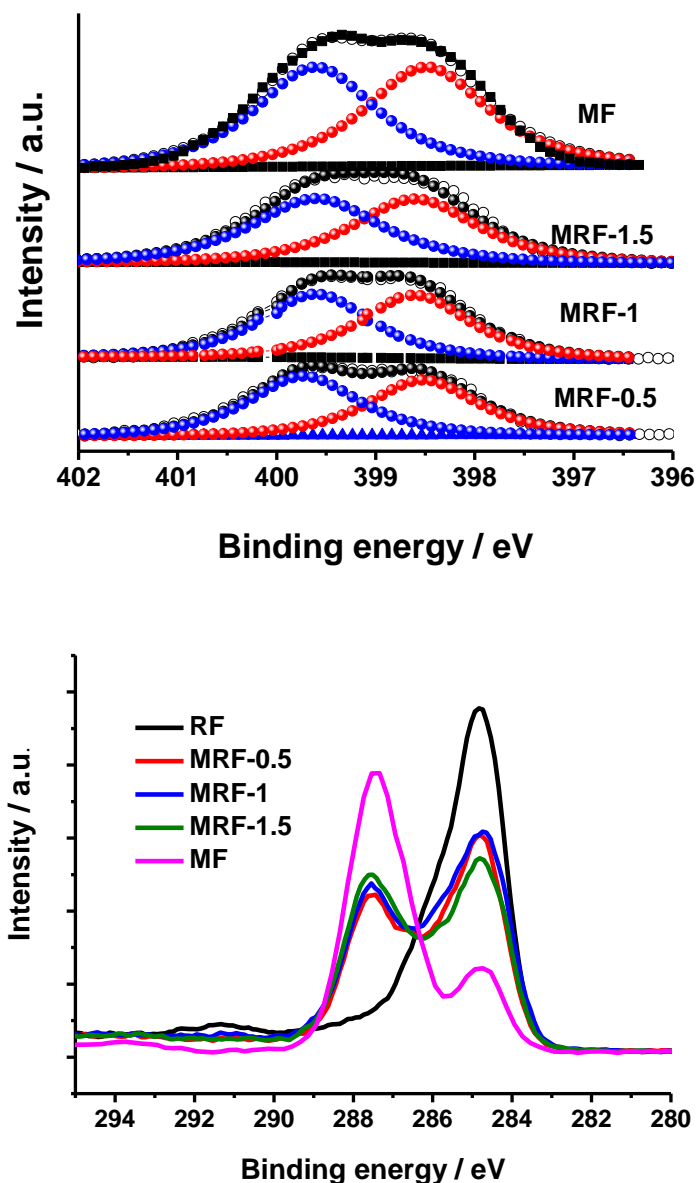


Fig. S2 XPS N1S and C1S spectra of the MRF microspheres. The XPS N1s spectra were deconvoluted into two peaks with binding energies of 398.4 and 399.6 eV that corresponded to the neutral imine nitrogen atoms (C-NH-C) and triazine nitrogen atoms (C=N-C), respectively. The relative intensities of these two peaks are almost similar, which can only result from melamine as the nitrogen source.

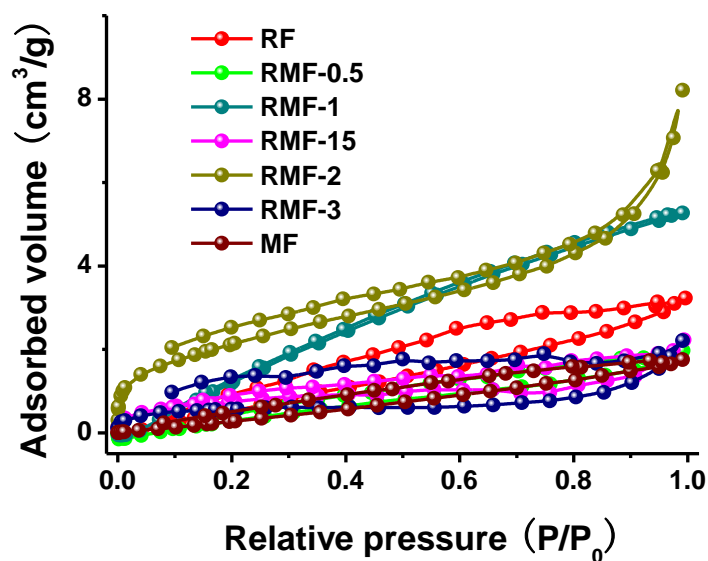


Fig. S3 N₂ adsorption-desorption isotherms of MRF microspheres at 77K. The obtained isotherms are classical type III according to the IUPAC classification, indicating only slight surface adsorption. Nevertheless, N₂ adsorption at 77 K is the most widely used and, sometimes, it is applied as a routine technique to obtain abundant information. However, its main disadvantage is that, at 77 K, the low relative pressure range (10^{-3} – 10^{-8}) data are not useful, because severe diffusional problems of the molecules inside the narrow pores (<0.7 nm).

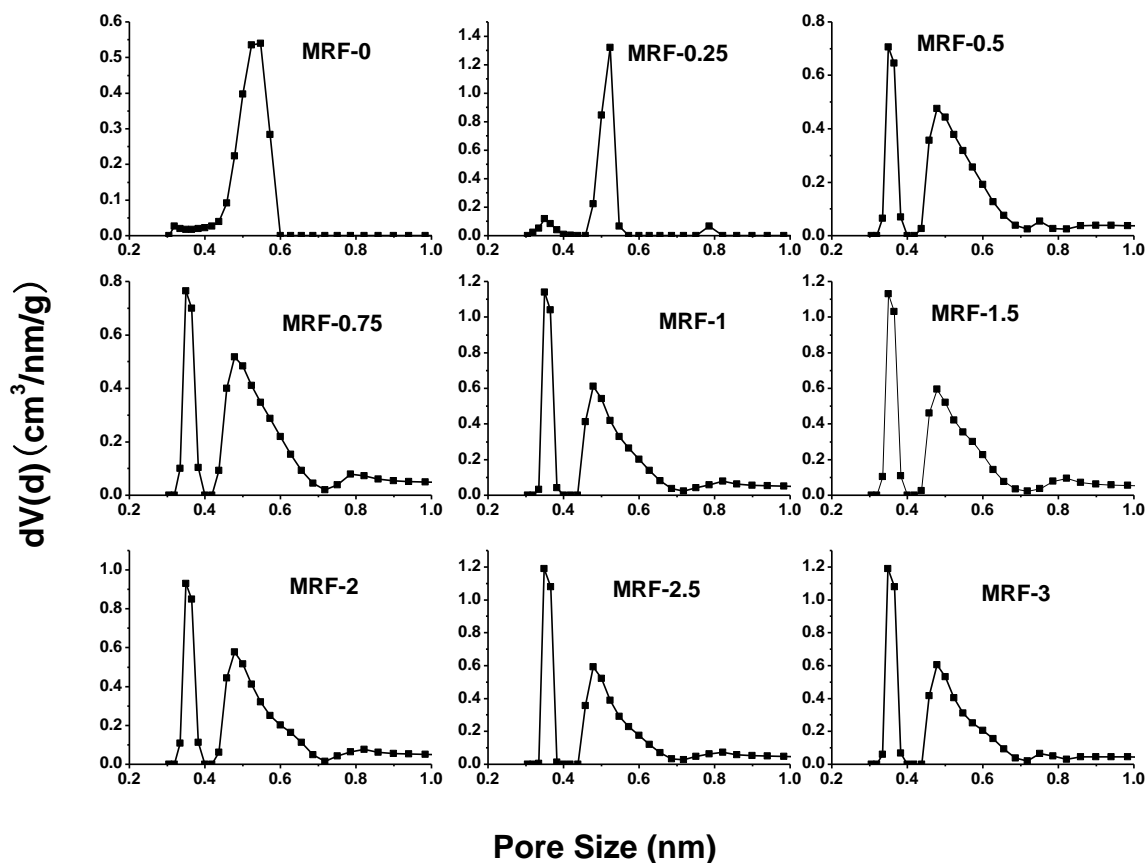


Fig. S4 NFDFT pore size distribution of MRF microspheres derived from CO₂ adsorption isotherms at 273 K. The M-free RF network shows a narrow unimodal peak at around 0.4–0.6 nm. The addition of M into RF network could broaden the peak of RF network into the range of 0.4–0.7 nm. Meanwhile, a new narrow peak, located at 0.3–0.4 nm presents for all M-contained MRF microspheres.

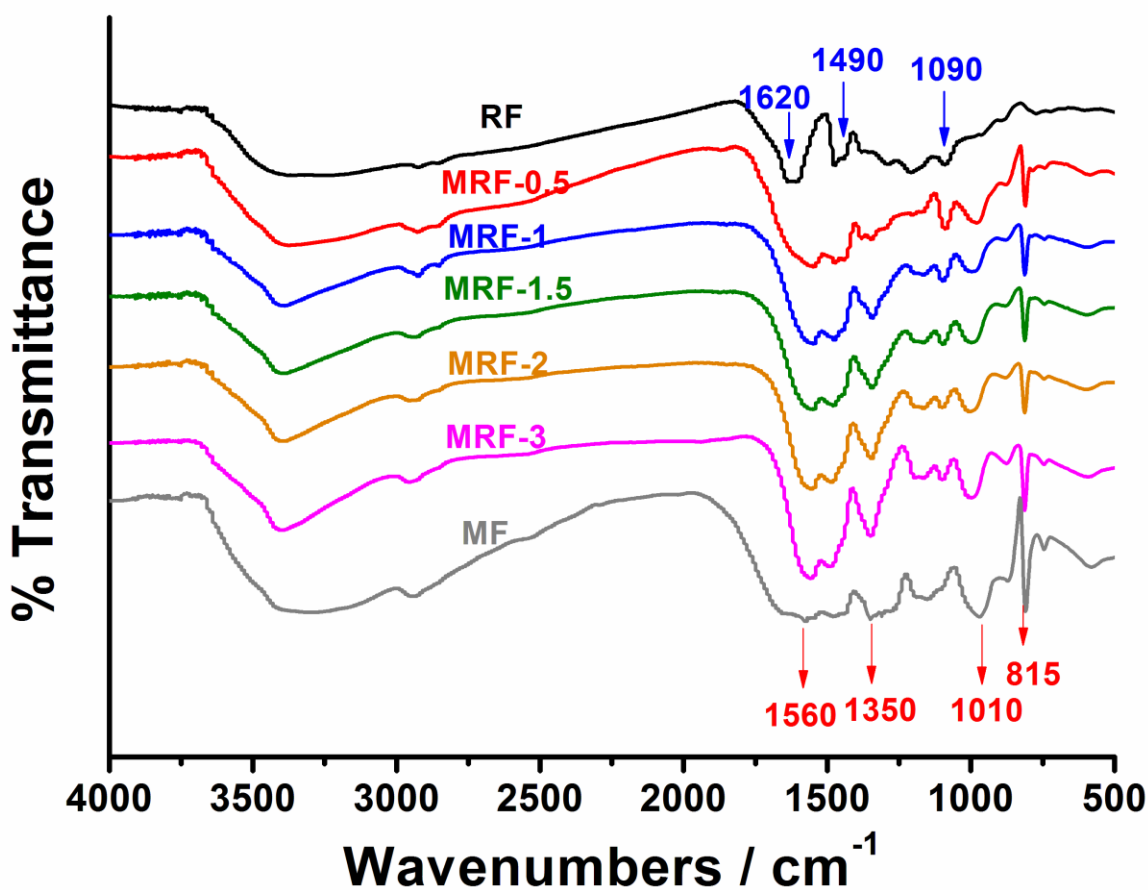


Fig. S5 The FTIR spectra of MRF microspheres with different M/R ratios. The successful incorporation of M into RF network is also indicated by FTIR spectra (Fig. 2b), in which the two strong absorption bands at 1558 and 1350 cm⁻¹ represent the aromatic C–N stretching and “breathing” modes in the triazine unit, respectively, which do not appear in the M-free RF sample. In addition, the typical C=C stretching vibrations at 1620 and 1490 cm⁻¹ present for all MRF microspheres, which do not appear in the R-free MF sample.

Table S1 CHN analysis and theoretical composition of MRF microspheres

Samples	Theoretical value		CHN analysis				
	N	N/C	N/C	N	C	H	O
	wt. %	at./at.	at./at.	wt. %	wt. %	wt. %	wt. %
MRF-0	0	0	0	0	60.19	3.48	33.67
MRF-0.25	10.5	0.16	0.15	10.35	57.9	4.42	27.31
MRF-0.5	17	0.27	0.27	16.45	53.01	4.62	25.92
MRF-1	24.6	0.47	0.43	26.02	46.07	4.69	23.22
MRF-1.5	28.9	0.55	0.53	28.08	43.82	4.62	23.48
MRF-2	31.6	0.63	0.6	30.72	41.96	4.65	22.67
MRF-2.5	33.6	0.68	0.65	33.62	42.41	4.74	19.23
MRF-3	35	0.73	0.69	34.16	40.01	4.77	21.06
MF	44.67	1	1.04	44.55	36.52	5.10	13.83

Table S2 Pore parameters of MRF microspheres calculated from N₂ and CO₂ isotherms

Samples	$S_{\text{BET}}^{\text{a}}$ (m ² /g)	$S_{\text{BET}}^{\text{b}}$ (m ² /g)	$S_{\text{DFT}}^{\text{c}}$ (m ² /g)	$V_{\text{DFT}}^{\text{d}}$ (cm ³ /g)	Dp^{e} (nm)
RF	5	128	205	0.052	0.55
MRF-0.25	3.1	159	240	0.069	0.52
MRF-0.5	2.9	285	440	0.116	0.35
MRF-0.75	4.2	346	512	0.138	0.35
MRF-1	4.6	372	509	0.146	0.35
MRF-1.5	2.8	395	590	0.156	0.35
MRF-2	3.4	376	549	0.145	0.35
MRF-2.5	7.8	353	522	0.138	0.35
MRF-3	2.8	357	561	0.144	0.35
MF	3.4	-	-	-	-

^a BET surface area calculated from N₂ adsorption isotherms at 77K; ^b BET surface area calculated from CO₂ adsorption isotherms at 273 K; ^c DFT surface area calculated from CO₂ adsorption isotherms at 273 K; ^d DFT pore volume calculated from CO₂ adsorption isotherms at 273 K; ^e average pore diameter calculated from CO₂ adsorption isotherms at 273 K.

Table S3 Pore parameters of MRF microspheres calculated from N₂ and CO₂ isotherms

Network	S _{BET} ^a m ² /g	CO ₂ uptake mmol/g	T (K)	P (bar)	Ref.
MRF-0	128	0.9	273	1	This work
MRF-0.5	285	1.89	273	1	
MRF-1	371	2.39	273	1	
MRF-1.5	395	2.54	273	1	
MRF-2	376	2.52	273	1	
MRF-3	357	2.42	273	1	
MOP-A	4077	2.65	273	1	1
MOP-B	1213	2.42	273	1	1
MOP-C	1470	2.55	273	1	1
MOP-D	1056	2.15	273	1	1
HCP 1	1646	3.01	273	1	2
HCP 3	1531	3.25	273	1	2
COF-1	750	2.32	273	1	3
COF-8	1350	1.43	273	1	3
COF-10	1760	1.21	273	1	3
COF-102	3620	1.56	273	1	3
PAF-1	5600	2.05	273	1	4
PAF-4	2246	2.41	273	1	4
CMP-1	837	2.05	273	1	5
CMP-1-(OH) ₂	1043	1.8	273	1	5
CMP-1-(CH ₃) ₂	899	1.64	273	1	5
Tet1	3160	2.55	273	1	6
Tet2	1102	1.96	273	1	6
POF1B	917	2.14	273	1	7

^a BET surface areas in this work were calculated from CO₂ adsorption isotherms at 273 K

References

- 1 R. Dawson, E. Stöckel, J. R. Holst, D. J. Adams and A. I. Cooper, *Energy Environ. Sci.*, 2011, 4, 4239.
- 2 C. F. Martin, E. Stöckel, R. Clowes, D. J. Adams, A. I. Cooper, J. J. Pis, F. Rubiera and C. Pevida, *J. Mater. Chem.*, 2011, 21, 5475–5483.
- 3 H. Furukawa and O. M. Yaghi, *J. Am. Chem. Soc.*, 2009, 131, 8875–8883.
- 4 T. Ben, H. Ren, S. Q. Ma, D. P. Cao, J. H. Lan, X. F. Jing, W. C. Wang, J. Xu, F. Deng, J. M. Simmons, S. L. Qiu and G. S. Zhu, *Angew. Chem., Int. Ed.*, 2009, 48, 9457–9460.
- 5 R. Dawson, D. J. Adams and A. I. Cooper, *Chem. Sci.*, 2011, 2, 1173–1177.
- 6 J. R. Holst, E. Stöckel, D. J. Adams and A. I. Cooper, *Macromolecules*, 2010, 43, 8531–8538.
- 7 A. P. Katsoulidis and M. G. Kanatzidis, *Chem. Mater.*, 2011, 23, 1818–1824.